

# Obtaining single path phase delays from GPS double differences

Chris Alber, Randolph Ware, Christian Rocken, John Braun

University Corporation for Atmospheric Research (UCAR), Boulder, Colorado 80307

**Abstract.** We describe a method for obtaining single-path phase delays from GPS double differences. The resulting "zero differences" (ZDs) can be used for remote sensing of atmospheric water vapor. The method is demonstrated by simulating and observing atmospheric delay gradients, and by comparing ZDs with pointed radiometer observations of integrated water vapor along GPS ray paths. In-situ GPS antenna phase center and multipath effects are mapped in ZD residuals for a specific site and network. We conclude that ZDs derived from GPS network data show promise for real time sensing of water vapor for use in meteorological modeling and forecasting.

## Introduction

Global Positioning System (GPS) signals are delayed by propagation through the Earth ionosphere and neutral atmosphere. The delay is defined as the excess propagation path from the satellite to the receiver compared to travel through a vacuum. Ionospheric delays are dispersive and thus can be corrected using dual frequency GPS observations. Neutral atmospheric delays can be divided into hydrostatic (dry) and wet delay terms. The dry delay, based on the assumption of hydrostatic equilibrium, can be computed using surface pressure [Bevis *et al.*, 1992] or meteorological model information [Chen and Herring, 1997]. The total delay minus the dry delay gives the wet delay.

Using this approach, precipitable water vapor (PW) above the GPS antenna can be estimated with better than 2 mm accuracy [Duan *et al.*, 1996]. PW is estimated as the average vertical component of the integrated water vapor along the line-of-sight to each of the observed GPS satellites. Real time PW measurements derived from GPS network data are described by Rocken *et al.*, [1997]. More detailed measurements can be obtained by estimating the integrated water vapor ("slant water", or SW) along the GPS ray paths [Ware *et al.*, 1997]. Examples of real-time PW and post-processed SW are available via [www.gsl.ucar.edu/gpsnet/realtime.html](http://www.gsl.ucar.edu/gpsnet/realtime.html).

High accuracy GPS applications commonly use double differences to cancel satellite and receiver clock errors and to help determine integer values of GPS car-

rier phase ambiguities. However, since the double differences include observations along 4 different paths (from 2 observation sites to 2 satellites), they are more difficult to interpret than single path delays. In this paper we describe a method for converting double differences into single path phase delays (ZDs).

## Obtaining Zero Differences from Double Differences

Double differencing is widely used to analyze GPS observations. Let  $\phi_1^A$  and  $\phi_2^A$  be observations of satellites 1 and 2 by receiver A, and  $\phi_1^B$  and  $\phi_2^B$  be observations by receiver B. These observations can then be combined into single differences ( $s_1^{AB}$  and  $s_2^{AB}$ ), defined as

$$s_1^{AB} = \phi_1^A - \phi_1^B \quad \text{and} \quad s_2^{AB} = \phi_2^A - \phi_2^B \quad (1)$$

A double difference can be expressed as the difference of two single differences

$$dd_{12}^{AB} = (\phi_1^A - \phi_1^B) - (\phi_2^A - \phi_2^B) = s_1^{AB} - s_2^{AB} \quad (2)$$

Common mode errors in GPS observations cancel in double differencing. Primarily, this includes errors from satellite and receiver clocks. Depending on the equipment used and the network size, errors from satellite orbits, atmospheric delay, site coordinates, antenna phase center variations, and multipath effects may or may not difference out.

To convert double differences to single differences, we write the double differences,  $dd$ , as the product of a matrix  $D$  and a vector of single differences,  $s$ ,

$$Ds = dd \quad (3)$$

For an individual baseline and  $n$  single differences, there are only  $n-1$  linearly independent double differences, and  $D$  cannot be inverted. However, if we introduce an additional independent constraint on at least one of the single differences, as shown in Equation (4), then  $D$  has a well defined inverse. The additional constraint is expressed at the upper right as a weighted sum of the single differences between sites  $I$  and  $J$  at one observation epoch. The satellite-dependent weighting for the site pair  $IJ$  is  $w_{ij}$ .  $\sum w_{ij} s_i^{IJ}$  can be estimated using model parameters from the GPS analysis, or by using a pointed water vapor radiometer (WVR) with a barometer or model for total delay estimation.

$$\begin{bmatrix} w_1 & w_2 & w_3 & \dots & w_n \\ 1 & -1 & 0 & \dots & 0 \\ 1 & 0 & -1 & \dots & 0 \\ \dots & \dots & \dots & \dots & \dots \\ 1 & 0 & 0 & \dots & -1 \end{bmatrix} \begin{bmatrix} s_1 \\ s_2 \\ s_3 \\ \dots \\ s_n \end{bmatrix} = \begin{bmatrix} w_1 s_1 + \dots + w_n s_n \\ s_1 - s_2 \\ s_1 - s_3 \\ \dots \\ s_1 - s_n \end{bmatrix} = \begin{bmatrix} \Sigma w_i s_i \\ dd_{12} \\ dd_{13} \\ \dots \\ dd_{1n} \end{bmatrix} \quad (4)$$

If we model all GPS observation effects and use the post-fit double difference residuals in Equation (4), then setting  $\Sigma w_i s_i$  equal to zero (the “zero mean” assumption) produces an inverse where the single differences retain the un-modeled part of the double differences. Included in these single differences are effects such as multipath or tropospheric inhomogeneities. The constraint can be improved by downweighting the single differences at low angles.

We obtain zero differences using all single differences to a given satellite from all linearly independent site pairs in the GPS network. Starting with Equation (5)

$$D_i z_i = s_i \quad (5)$$

where  $D_i$  is a matrix operating on a vector of zero differences for the  $i$ 'th satellite,  $z_i$ , to produce the vector of single differences  $s_i$ . We obtain a form for  $D_i$  including an additional constraint (upper right) on the zero differences in Equation (6)

$$\begin{bmatrix} w_A & w_B & w_C & \dots & w_Z \\ 1 & -1 & 0 & \dots & 0 \\ 1 & 0 & -1 & \dots & 0 \\ \dots & \dots & \dots & \dots & \dots \\ 1 & 0 & 0 & \dots & -1 \end{bmatrix} \begin{bmatrix} z_A \\ z_B \\ z_C \\ \dots \\ z_Z \end{bmatrix} = \begin{bmatrix} w_A z_A + \dots + w_Z z_Z \\ z_A - z_B \\ z_B - z_C \\ \dots \\ z_A - z_Z \end{bmatrix} = \begin{bmatrix} \Sigma w_i z_i \\ s_{AB} \\ s_{BC} \\ \dots \\ s_{AZ} \end{bmatrix} \quad (6)$$

The weighting for the  $i$ 'th satellite at the  $i$ 'th site is  $w_i$ , and  $\Sigma w_i z_i$  includes single path effects to the  $i$ 'th satellite from each site. As before, we can downweight the zero differences used in the constraint at low elevation angles. If we assume that  $\Sigma w_i z_i$  equals zero, we can obtain zero differences which represent the slant delay fluctuations about the model used to obtain the double and single differences.

In both inversions, any error in the zero-mean assumption is divided equally over all stations in the network. For example, if for a 10 site network a 10 mm delay is present in one ZD, the mean residual will have a 1-mm error. The ZDs are relative to the ensemble mean of the network. This implies that large networks can be used with careful modeling to minimize biases. Station coordinates should be held fixed to known long-term averages to avoid correlation with slant delays.

For tropospheric slant delays, the zero mean assumption implies that the residual delay in the direction of one GPS satellite at each epoch, averaged over the entire GPS network, is equal to zero. For a GPS network that

is distributed over a large area ( $\sim 100$  km), this assumption is generally valid because the distribution of water vapor at the sites can be considered random and the mean zenith delay can be estimated and removed. For a small network, if all stations observe a satellite through the same volume of atmosphere, the delay will have common mode elements that cannot be resolved. One method to compute absolute slant delays for a small network uses a collocated pointed radiometer and barometer (or modeled pressure fields) at one site. Absolute slant delay calculated from the wet and dry delay measurements at the collocated site can be used to lever absolute slant delays at the other sites. Another method is to analyze the small network within a larger network to minimize common mode error.

### Single Path Delay Simulation and Observation

We demonstrate the zero difference method using synthetic GPS data including 1-mm phase noise and a  $\pm 10$  mm delay gradient from east to west at 10 degrees elevation (Figure 1). The gradient was applied to one of eight network sites in Colorado, Kansas and Oklahoma (<http://www.dd1sl.noaa.gov/gps.html>).

The zero-mean assumption was violated in the simulated data since the gradient delay was added to only one site -- data for the other seven sites included noise only. Therefore, the retrieved ZD observations from each site contained  $\pm 10/8 = \pm 1.2$  mm error. The right panel shows observed ZD variations over a 2-hour time period at Platteville, Colorado, using the same eight site network. The simulated gradient is similar in magnitude (but opposite in sign) to the observed gradient. Bernese GPS software [Rothacher and Mervart, 1996] was used to process the simulated and observed data. The ZD method was used to extract slant delays from the Bernese DD residuals.

### Sensing Integrated Water Vapor Along GPS Ray Paths

The ZD method can be used to sense variations in atmospheric water vapor along GPS ray paths. This is

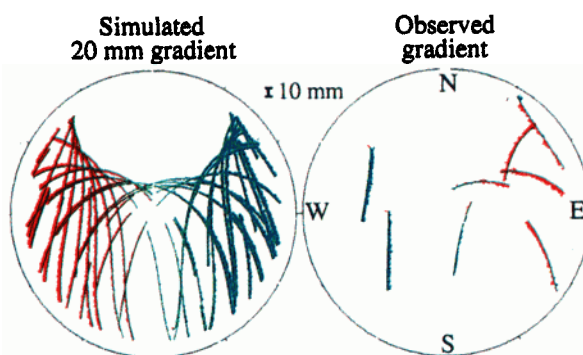


**Figure 1.** Simulated (24-hr) and observed (2-hr) ZDs vs. satellite elevation and azimuth angle (“sky plots”). Plot center is zenith and right center the eastern horizon. Red (negative) and blue (positive) residuals are plotted relative to satellite ground tracks (light green).

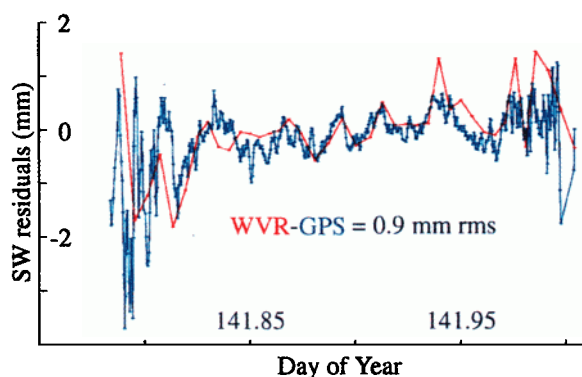


**Figure 2.** Comparison of GPS-sensed (ZD method) and WVR-sensed SW above 10 degrees elevation. Sampling intervals are 8 min (WVR) and 30 sec (GPS).

demonstrated by comparing 8-min pointed radiometer and 30-sec ZD sensed SW in Figure 2. Once again, we use GPS data from the eight site network. The residuals are total SW minus 30-min PW mapped to the elevation angle. Good agreement (0.9 mm rms) is seen between the two measurements. *Braun et al.* [2000] made a similar comparison using three days of data and found 0.7 mm rms agreement above 20 degrees elevation. For the same data set, *Ware et al.* [1997] found 1.3 mm rms agreement between double difference pointed radiometer and GPS residuals. This corresponds to 0.6 mm rms (RSS) agreement for each of the 4 ZDs in the double difference residuals. The zero mean assumption is the only additional error introduced in deriving ZDs from the double differences. We therefore conclude that the error resulting from this assumption is relatively small for this case.

It is evident from Figure 2 that the ZD SW noise level decreases at high elevation angles near plot center. Similarly, *Braun et al.* [2000] found that the ZD SW noise level is 0.2 mm rms near zenith and 1.4 mm rms near 10 degrees elevation. We attribute the large oscillations in the GPS residual at low angles (both ends of the plot) to ground-scattered multipath.

ZD sensed SW data show promise for meteorological applications. *MacDonald and Xie* [2000] simulated the use of SW data from a GPS network with 40-km spacing. They found that high resolution 3D humidity fields could be determined from SW data. They concluded that assimilation of SW data into weather models should provide significant improvements in forecasting. A variety of meteorological (and other) applications for single path GPS residuals are described by *Ware et al.* [2000].

### Mapping Antenna Effects in ZD Residuals

We apply the ZD method to data from four GPS receivers with their antennas located on the corners of a 10 m square at Table Mountain, Colorado. Three of the antennas were designed for minimal phase center variations. The fourth antenna was an Allen Osborne and Associates Dorne Margolin choke ring. A map of the

ZD residuals for the Dorne-Margolin antenna is shown in Figure 3. The ZD phase center variations are relative to the mean phase center pattern of the ensemble of antennas. In general, this mean was not zero. However, this map is similar to the phase center pattern determined from anechoic chamber tests [*Meertens et al.*, 1996] which is also shown. In-situ phase center variations of Dorne Margolin antennas are currently under debate within the International GPS Service (IGS) community. Figure 3 shows in-situ antenna phase variations similar to anechoic chamber measurements. The in-situ results can be used to correct antenna phase center effects in ZD residuals for specific networks and sites.

### Mapping Multipath Effects in ZD Residuals

Residual phase variations that repeat with the periodicity of the GPS orbits (sidereal time) can be mapped with the ZD method. Assuming that site coordinates, carrier phase ambiguities, GPS orbits, in-situ antenna phase center variations, and mean atmospheric delay are all accurately modeled, the ZD residuals are dominated by the un-modeled atmospheric slant delay and ground-scattered multipath. Un-modeled atmospheric delay varies on a daily basis, but the multipath tends to repeat in sidereal time. Detailed multipath maps can be computed by “stacking” daily GPS residuals. Daily residuals, a 21-day stacked multipath map, and a corrected set of residuals are shown for a single frequency site [*Braun et al.*, 1999]. Multipath effects can be corrected by subtracting the stacked multipath map from the residuals. The reduction of multipath error, particularly at low elevation angles, is evident in the corrected plot. Residual variations are reduced from 3.8 to 2.5 mm rms over all angles. Stacking of residuals allows for the separation of multipath and unmodeled atmospheric slant delay.

### Conclusions

The ZD method obtains single path phase delays from double differences. The resulting residuals can be

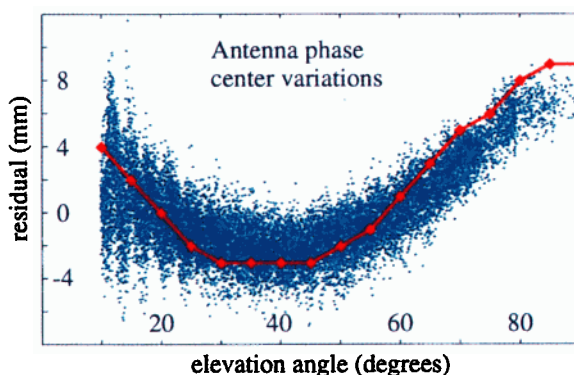


**Figure 3.** Dorne-Margolin phase center and multipath map in ZD residuals (blue) compared with anechoic chamber measurements (red). We attribute the modulation in the ZD residuals at low elevations to ground-scattered multipath.

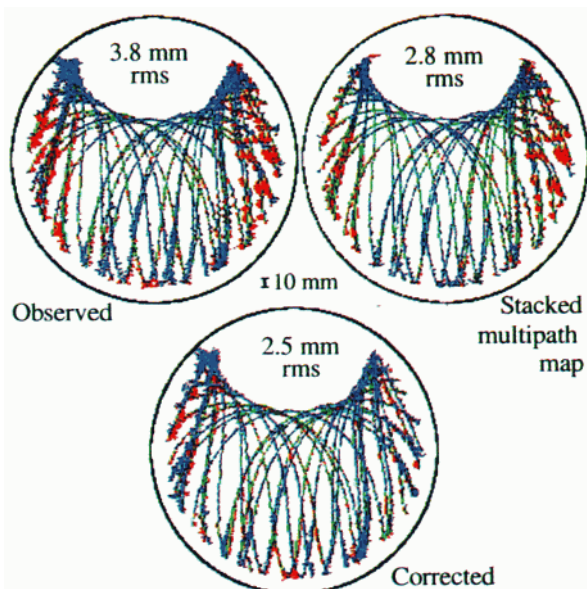


**Figure 4.** ZD corrections at Lamont, Oklahoma, obtained by subtracting the multipath map from the observed 24-hr ZDs (sky plots similar to Figure 1).

used to sense integrated water vapor along GPS ray paths. The ZD method assumes a “zero mean” assumption to derive single and zero differences from double differences. During a three day test, we showed that the error in the ZD residuals resulting from this assumption is relatively small. We also showed that errors resulting from antenna phase center and ground-scattered multipath effects in ZD residuals can be mapped and corrected for specific networks and sites. Overall, the ZD method shows promise for real time sensing of atmospheric water vapor in meteorological applications.

**Acknowledgments:** This work was supported by the Office of Naval Research, Dr. Scott Sandgathe, Code 322MM, and by the Department of Energy Atmospheric Radiation Measurement (ARM) Batelle grant 354106-AQ5. GPS network data were provided by NOAA’s Forecast Systems Laboratory.

## References

- Bevis, M., S. Businger, T. Herring, C. Rocken, R. Anthes, and R. Ware, GPS Meteorology: Remote Sensing of Atmospheric Water Vapor using the Global Positioning System, *J. Geophys. Res.*, **97**, 15,787–15,801, 1992.
- Braun, J., C. Rocken, and R. Ware, Operating a dense L1 GPS network for atmospheric sensing, *EOS, Trans. Am. Geophys. Union*, **80**, G12A-09, 1999.
- Braun, J., C. Rocken, and R. Ware, Validation of single slant water vapor measurements with GPS, *Rad. Sci.* (submitted), 2000.
- Chen, G., and T. Herring, Effects of atmospheric azimuthal asymmetry on the analysis of space geodetic data, *J. Geophys. Res.*, **102**, 20,489–20,502, 1997.
- Duan, J., and Coauthors, GPS Meteorology: direct estimation of the absolute value of precipitable water, *J. Appl. Meteor.*, **35**, 830–838, 1996.
- MacDonald, A., and Y. Xie, On the Use of Slant Observations from GPS to Diagnose Three Dimensional Water Vapor Using 3DVAR, Proc. 4th Integrated Observing Systems Symp. (Amer. Met. Soc.), Long Beach CA, 62–73, 2000.
- Meertens, C., and Coauthors, Antenna Type, Mount, Height, Mixing and Snow Effects in High Accuracy GPS Observations, GPS for the Geosciences: Workshop Proceedings, National Academy Press ([www.nap.edu/books/N0004211.html](http://www.nap.edu/books/N0004211.html)), 211–218, 1997.
- Rocken, C., T. Van Hove and R. Ware, Near real-time GPS sensing of atmospheric water vapor, *Geophys. Res. Lett.*, **24**, 3221–3224, 1997.
- Rothacher, M., and L. Mervart (editors), Bernese GPS Software Version 4.0, Astronomical Institute, Univ. Berne, 1996.
- Ware, R., C. Alber, C. Rocken and F. Solheim, Sensing integrated water vapor along GPS ray paths, *Geophys. Res. Lett.*, **24**, 417–420, 1997.
- Ware, R., and Coauthors, SuomiNet: A Real-Time National GPS Network for Atmospheric Research and Education, *Bull. Am. Met. Soc.*, **81**, 677–694, 2000.
- C. Alber, R. Ware, C. Rocken, and J. Braun, University Corporation for Atmospheric Research, Boulder, CO, 80307. (e-mail: ware@ucar.edu)

(Received February 24, 2000; revised May 13, 2000; accepted June 19, 2000)